Inorg. Chem. **2005**, *44*, 7365–7376

New Palladium(II) and Platinum(II) Complexes with the Model Nucleobase 1-Methylcytosine: Antitumor Activity and Interactions with DNA

José Ruiz,* Natalia Cutillas, Consuelo Vicente, María Dolores Villa, and Gregorio López

Departamento de Química Inorgánica, Facultad de Química, Universidad de Murcia, 30071 Murcia, Spain

Julia Lorenzo and Francesc X. Avilés

Institut de Biotecnología i Biomedicina, Department de Bioquímica i de Biología Molecular, Universitat Autònoma de Barcelona, 08193 Barcelona, Spain

Virtudes Moreno

Department de Química Inorgànica, Universitat de Barcelona, Martí i Franquès 1-11, 08028 Barcelona, Spain

Delia Bautista

S.U.I.C., Edificio S.A.C.E., Universidad de Murcia, 30071-Murcia, Spain

Received February 15, 2005

Palladium and platinum complexes with the model nucleobase 1-methylcytosine (1-Mecyt) of the types [Pd(N–N)(C_6F_5)(1-Mecyt)]ClO_4 [N–N = bis(3,5-dimethylpyrazol-1-yl)methane (bpzm*), bis(pyrazol-1-yl)methane (bpzm), *N*,*N*,*N*′,*N*′-tetramethylethylenediamine (tmeda), or 2,2′-bipyridine (bpy)] and [M(dmba)(L′)(1-Mecyt)]ClO_4 [dmba = *N*,*C*-chelating 2-(dimethylaminomethyl)phenyl; L′ = PPh_3 (M = Pd or Pt), DMSO (M = Pt)] have been obtained. Palladium and platinum complexes of the types *cis*-[M(C_6F_5)$_2$(1-Mecyt)$_2$] (M = Pd or Pt) and *cis*-[Pd(L′)(C_6F_5)(1-Mecyt)$_2$]ClO_4 (L′ = PPh_3 or *t*-BuNC) have also been prepared. The crystal structures of [Pd(bpzm*)(C_6F_5)(1-Mecyt)]ClO_4, [Pt(dmba)(DMSO)(1-Mecyt)]ClO_4, *cis*-[Pd(C_6F_5)$_2$(1-Mecyt)$_2$], and *cis*-[Pd(*t*-BuNC)(C_6F_5)(1-Mecyt)$_2$]ClO_4 have been established by X-ray diffraction. There is extensive hydrogen bonding (N–H···O, C–H···F or C–H···O) in all the compounds. There are also intermolecular π–π interactions between pyrimidine rings of adjacent chains in [Pd(C_6F_5)$_2$(1-Mecyt)$_2$]. DNA adduct formation of the new complexes synthesized was followed by circular dichroism and electrophoretic mobility. Atomic force microscopy images of the modifications caused by the complexes on plasmid DNA pB*R*322 were also obtained. Values of IC_{50} were also calculated for the new complexes against the tumor cell line HL-60. At a short incubation time (24 h) almost all new complexes were more active than cisplatin.

Introduction

Today platinum complexes are some of the most promising drugs in chemotherapy.[1,2] Genomic DNA is generally accepted as the main pharmacological target of cisplatin-induced cytotoxicity.[3,4] The major product of cisplatin interaction with DNA is a 1,2-intrastrand cross-link, which induces a kink on a DNA double helix.[3,5,6] However,

* To whom correspondence should be addressed. Fax: (+34) 968 36 41 48. E-mail: jruiz@um.es.

(1) *Cisplatin-Chemistry and Biochemistry of a leading Anticancer Drug*; Lippert, B., Ed.; Wiley-VCH: Weinheim, 1999.
(2) Wong, E.; Giandomenico, C. M. *Chem. Rev.* **1999**, *99*, 2451.
(3) Reedjik, J. *Chem. Commun.* **1996**, 801.
(4) Takahara, P. M.; Frederick, C. A.; Lippard, S. J. *J. Am. Chem. Soc.* **1996**, *118*, 12309.

10.1021/ic0502372 CCC: $30.25
Published on Web 09/13/2005

significant problems still exist, including side effects, toxicity, cancer specificity, and specially acquired resistance. Consequently, antitumor drug research has been moving toward the development of new compounds outside the usual coordination sphere, e.g., organometallic complexes[7] or complexes with metallic elements different from platinum. Because of the lanthanoid contraction, platinum and palladium both have nearly the same ionic radius (Pt(II) 0.74 Å, Pd(II) 0.78 Å). Accordingly, a very large similarity of both metals within their coordinative behavior can be observed, although their kinetic behavior with respect to ligand substitution is very different.

In the present study our initial aim was to synthesize organopalladium and organoplatinum complexes derived from the *N*,*C*-chelating 2-(dimethylaminomethyl)phenyl (dmba) and pentafluorophenyl groups with a representative model nucleobase, namely, 1-methylcytosine (1-Mecyt), which display rather versatile metal-ion binding patterns.[8] To our knowledge, the complexes reported herein represent the first examples of palladium and platinum complexes containing neutral 1-Mecyt and a σ-metal carbon bond. Some of these complexes have been characterized by X-ray diffraction. We also studied the interactions of these complexes with DNA by circular dichroism and electrophoretic mobility. Atomic force microscopy images of the modifications caused by the complexes on plasmid DNA pB*R*322 were also obtained. The in vitro antiproliferative activity of the new complexes in HL-60 cell line has been studied.

Scheme 1

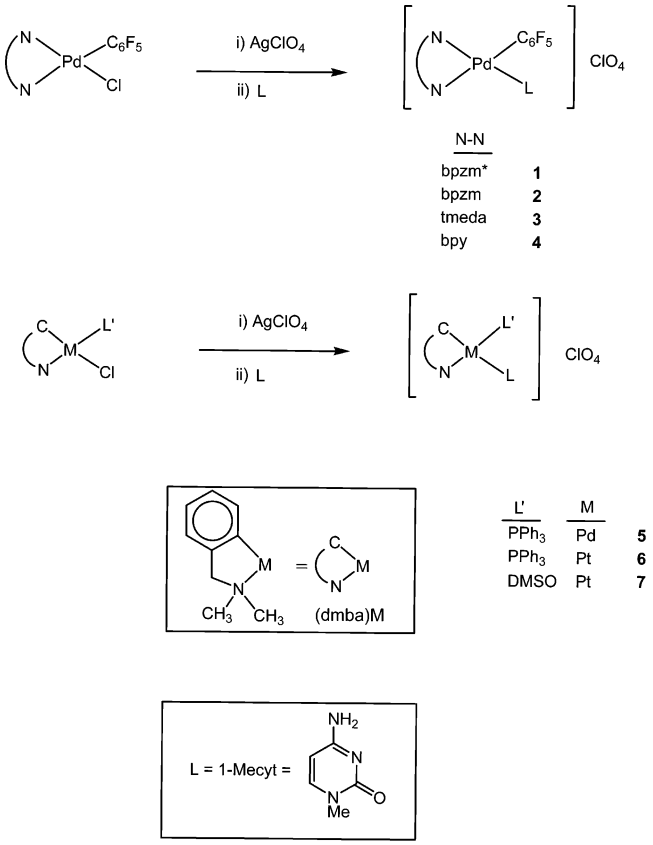

Results and Discussion

Complexes [Pd(N−N)(C_6F_5)(1-Mecyt)]ClO_4. In acetone, the solvento complexes [Pd(N−N)(C_6F_5)(Me_2CO)]ClO_4 [N−N = bis(3,5-dimethylpyrazol-1-yl)methane (bpzm*), bis(pyrazol-1-yl)methane (bpzm), *N*,*N*,*N*′,*N*′-tmeda (tetramethylethylenediamine), or bpy (2,2′-bipyridyl)] (prepared by reaction of the corresponding chloride derivatives [PdCl(C_6F_5)(N−N)] with $AgClO_4$ in a 1:1 molar ratio in acetone at room temperature) react with 1 equiv of 1-Mecyt to yield the corresponding cationic complexes [Pd(N−N)(C_6F_5)(1-Mecyt)]-ClO_4 (**1**−**4**) (Scheme 1) in 55−85% yields. The structures were assigned on the basis of microanalytical, IR, and ^{1}H and ^{19}F NMR data. Complexes **1**−**4** are all air-stable solids, and thermal analysis shows that they decompose above 230 °C in a dynamic N_2 atmosphere. Their acetone solutions show conductance values corresponding to 1:1 electrolytes (Λ_M in the range 132−152 S cm^2 mol^{-1}).[9] Two IR bands are observed at ca. 1090 and 1050 cm^{-1}; one is assigned to the ν_3 mode of free perchlorate (T_d symmetry) and the other to a vibrational mode of the C_6F_5 group. The observation of an additional band at ca. 623 cm^{-1} for the ν_4 mode confirms the presence of free perchlorate.[10] The IR spectra show the characteristic absorptions of the C_6F_5 group[11] at 1630, 1490, 1450, 1050, and 950 and a single band at ca. 800 cm^{-1} derived from the so-called X-sensitive mode[12] in C_6F_5X (X = halogen) molecules, which is characteristic of the presence of only one C_6F_5 group in the coordination sphere of the palladium atom and behaves like a ν(M−C) band.[13] The characteristic resonances of the chelate ligands are observed in the ^{1}H NMR spectra,[14−17] and the assignments presented in the Experimental Section are based on the atom numbering given in Scheme 2. In complexes **1** and **2** two sets of ^{1}H resonances are observed for the $C_3HMe_2N_2$ or $C_3H_3N_2$ rings corresponding to one pyrazolate ligand trans to 1-Mecyt and one pyrazolate ligand trans to C_6F_5. The proton resonances of the bridging methylene of the bis(pyrazol-1-yl)methane ligands in complexes **1** and **2** show that the boat-to-boat inversion usually observed in this type of complex[14] is frozen at room temperature; the methylene protons are magnetically nonequivalent and give an NMR pattern corresponding to two diastereotopic protons: two doublets with $^2J_{H_AH_B} \approx 15$

(5) Guo, Z. J.; Sadler, P. J. *Angew. Chem., Int. Ed. Engl.* **1999**, *38*, 1513.
(6) Jamieson, E. R.; Lippard, S. J. *Chem. Rev.* **1999**, *99*, 2467.
(7) Fish, R. H.; Jaouen, G. *Organometallics* **2003**, *22*, 2166.
(8) Lippert, B. *Coord. Chem. Rev.* **2000**, *200*−*202*, 487.
(9) Geary, W. J. *Coord. Chem. Rev.* **1971**, *7*, 81.
(10) Nakamoto, K. *Infrared and Raman Spectra of Inorganic and Coordination Compounds*, 5th ed.; Wiley-Interscience: New York, 1997; p 199.
(11) Long, D. A.; Steele, D. *Spectrochim. Acta* **1963**, *19*, 1955.
(12) Maslowski, E. *Vibrational Spectra of Organometallic Compounds*; Wiley: New York, 1977; p 437.
(13) Alonso, E.; Forniés, J.; Fortuño, C.; Tomás, M. *J. Chem. Soc., Dalton Trans.* **1995**, 3777.
(14) Ruiz, J.; Martínez, M. T.; Florenciano, F.; Rodríguez, V.; López, G.; Pérez, J.; Chaloner, P. A.; Hitchcock, P. B. *Inorg. Chem.* **2003**, *42*, 3650.
(15) Ruiz, J.; Martínez, M. T.; Florenciano, F.; Rodríguez, V.; López, G.; Pérez, J.; Chaloner, P. A.; Hitchcock, P. B. *Dalton Trans.* **2004**, 929.
(16) Byers, P. K.; Canty, A. J. *Organometallics* **1990**, *9*, 210.
(17) Forniés, J.; Martínez, F.; Navarro, R.; Urriolabeitia, E. P. *J. Organomet. Chem.* **1995**, *495*, 185.

Scheme 2

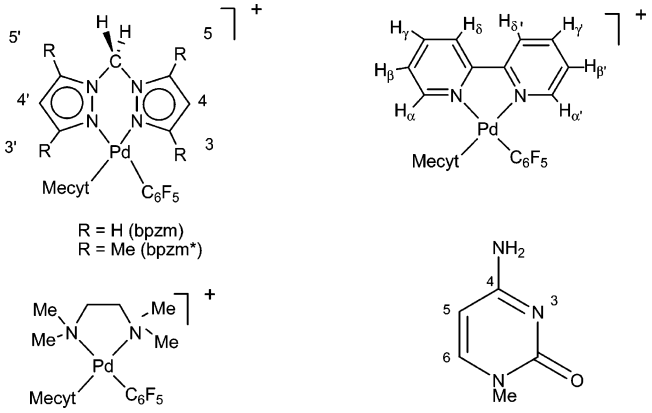

Hz. Figure 1 shows the variable-temperature ^{1}H NMR spectra of complex **1** in the N−CH_2−N region and the boat-to-boat inversion of the metallacycle Pd(N−N)$_2$C. In complexes **1**−**4** the H(5) and H(6) resonances of the 1-Mecyt ligand (Scheme 2) are shifted downfield by ∼0.1−0.2 ppm due to Pd binding, although the coupling constant between H(5) and H(6) was

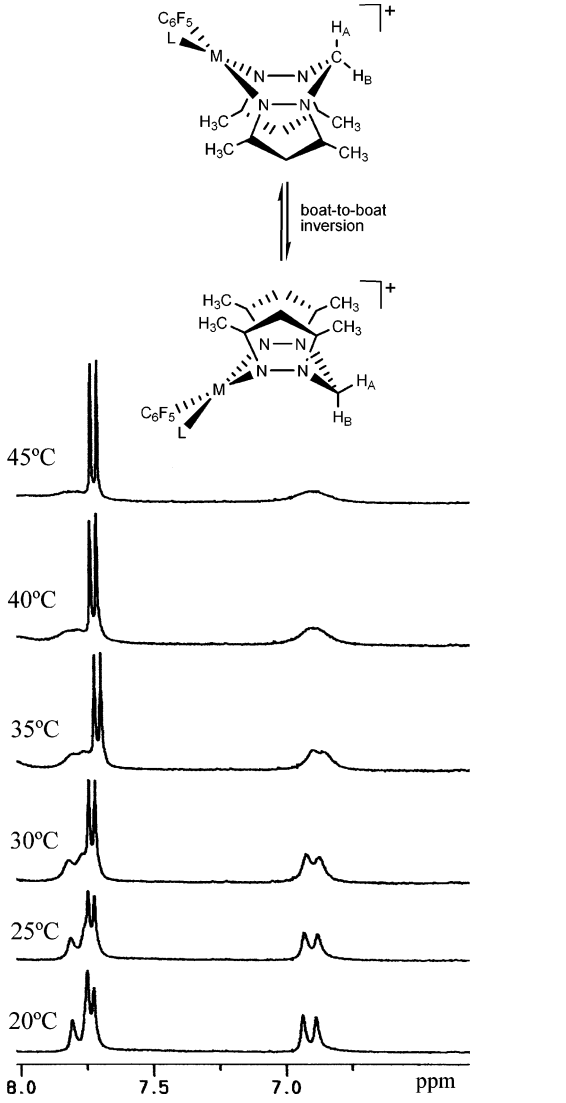

Figure 1. Variable-temperature ^{1}H NMR spectra of complex **1** in the N−CH_2−N region, and the boat-to-boat inversion of the metallacycle Pd(N−N)$_2$C.

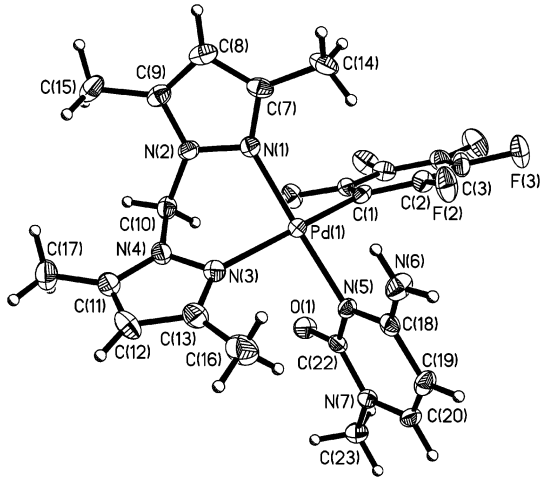

Figure 2. ORTEP of complex **1** showing the atom-numbering scheme. Displacement ellipsoids are drawn at the 50% probability level.

Table 1. Selected Bond Lengths and Angles for Complex 1

	bond lengths, Å		bond angles, deg	
molecule 1	Pd(1)−C(1)	1.988(4)	C(1)−Pd(1)−N(1)	91.21(13)
	Pd(1)−N(1)	2.031(3)	C(1)−Pd(1)−N(5)	88.01(12)
	Pd(1)−N(5)	2.044(3)	N(1)−Pd(1)−N(5)	178.02(12)
	Pd(1)−N(3)	2.131(3)	C(1)−Pd(1)−N(3)	167.48(13)
			N(1)−Pd(1)−N(3)	88.31(11)
			N(5)−Pd(1)−N(3)	92.86(11)
			C(22)−N(5)−C(18)	121.8(3)
molecule 2	Pd(2)−C(31)	2.004(4)	C(31)−Pd(2)−N(8)	90.83(13)
	Pd(2)−N(8)	2.015(3)	C(31)−Pd(2)−N(12)	90.90(12)
	Pd(2)−N(12)	2.034(3)	N(8)−Pd(2)−N(12)	177.17(12)
	Pd(2)−N(11)	2.090(3)	C(31)−Pd(2)−N(11)	168.72(13)
			N(8)−Pd(2)−N(11)	84.83(12)
			N(12)−Pd(2)−N(11)	93.06(11)
			C(48)−N(12)−C(52)	121.8(3)

unaffected (7.2 Hz). On the other hand, an interesting observation is that while the NH_2 of the free 1-Mecyt base is a broad singlet as is typically found for amino resonances which normally undergo free rotation on the NMR time scale, two NH resonances are observed for the coordinated 1-Mecyt ligand in complexes **1**−**4**. Both of these NH resonances are strongly shifted downfield (∼1.5−1.0 ppm) relative to the free base. The observation of two resonances is consistent with the intermolecular steric effects and hydrogen bonding observed in the solid state[18] (vide infra). The ^{19}F NMR spectra of complexes **1** and **3** reveal the presence of a freely rotating pentafluorophenyl ring which gives the expected three resonances (in the ratio 2:1:2) for the *o*-, *p*-, and *m*-fluorine atoms, respectively. The ^{19}F NMR spectra of complex **4** at room temperature show hindered rotation of the C_6F_5 ring around the Pd−C bond, and two separate signals are observed for the *o*- and *m*-fluorine atoms but only one for the *p*-fluorine atom.

Crystal Structure of 1. Figure 2 shows the X-ray structure of complex **1** with selected bond lengths and angles listed in Table 1. The crystal structure of compound **1** shows two independent molecules in the asymmetric unit with the palladium atoms in slightly distorted square-planar geometries. The different Pd−N (bpzm) distances (Pd(1)−N(1)

(18) Orbell, J. D.; Marzilli, L. G.; Kistenmacher, T. J. *J. Am. Chem. Soc.* **1981**, *103*, 5126.

Table 2. Hydrogen Bonds for Complex **1**[a]

D−H···A	*d*(D−H), Å	*d*(H···A), Å	*d*(D···A), Å	<(DHA), deg
N(6)−H(06B)···O(5)	0.89(3)	2.05(3)	2.938(4)	171(4)
N(13)−H(01A)···O(4)#1	0.89(3)	2.32(4)	2.962(5)	129(3)
C(53)−H(53A)···F(35)#2	0.98	2.38	3.250(5)	147.7
C(46)−H(46B)···F(35)#3	0.98	2.33	3.297(5)	167.7
C(50)−H(50)···O(4)#4	0.95	2.48	3.422(5)	169.2
C(23)−H(23C)···O(6)#5	0.98	2.54	3.461(5)	155.9
C(15)−H(15B)···O(5)#6	0.98	2.50	3.472(5)	171.9
C(23)−H(23B)···O(1)#7	0.98	2.40	3.383(5)	176.8

[a] Symmetry transformations used to generate equivalent atoms: #1 $x - 1/2, -y + 1/2, z + 1/2$; #2 $x + 1/2, -y + 1/2, z + 1/2$; #3 $-x + 3/2, y - 1/2, -z + 3/2$; #4 $x, y, z + 1$; #5 $x - 1/2, -y + 1/2, z - 1/2$; #6 $-x + 3/2, y - 1/2, -z + 1/2$; #7 $-x + 1, -y, -z$.

= 2.031(3) Å, Pd(1)−N(3) = 2.131(3) Å in molecule 1 and (Pd(2)−N(8) = 2.015 (3) Å, Pd(2)−N(11) = 2.090(3) Å in molecule 2) are in agreement with the higher trans influence of the C_6F_5 group compared with the 1-Mecyt ligand. The Pd−N(1-Mecyt) bond distance (Pd(1)−N(5) = 2.044(3) Å in molecule 1, Pd(2)−N(12) = 2.034(3) Å in molecule 2) is similar to the mean value of 2.040(7) Å found in the cation $[Pd(1\text{-Mecyt})_4]^{2+}$ [19] and slightly longer than 2.028(7) Å found in $[(trpy)Pd(1\text{-Mecyt})]^{2+}$.[20] Bond distances and angles within the 1-Mecyt molecule are in agreement with values previously reported for analogous ligands.[21] The 1-Mecyt ligand is planar, and the highest displacement from the least-squares plane defined by the six endocyclic atoms is 0.0323 Å for C(22) in molecule 1 and 0.0037 Å for C(51) in molecule 2. The 1-Mecyt plane is almost perpendicular to the coordination plane (dihedral angle between the planes is 91.9° in molecule 1 and 105.1° in molecule 2). The two C−N(5)−Pd angles are significantly different. The angle on the side of the NH_2 group (123.8(2)°) is larger than that on the O side (114.3(2)°). The two C−N(12)−Pd angles are also significantly different. The angle on the side of the NH_2 group (125.7(2)°) is larger than that on the O side (121.6-(2)°). The perchlorate anion conects two molecules through classical NH···O bonds. The nonclassical CH···O bonds link these molecules to form a three-dimensional network (Table 2). The chelate angle N(1)−Pd(1)−N(3) (88.31(11)°) in molecule 1 is larger than that found in molecule 2, N(8)−Pd(2)−N(3) (84.83(12)°).

Complexes [M(dmba)(L′)(1-Mecyt)]ClO_4. The dmba analogues of complexes **1**−**4** have been prepared from the corresponding precursor [MCl(dmba)(L′)] [L′ = PPh_3 (M = Pd or Pt), DMSO (M = Pt)]. After precipitation of AgCl by addition of $AgClO_4$ in a 1:1 molar ratio in acetone, the solvento complexes $[[M(dmba)(L')(Me_2CO)]ClO_4$ generated in situ react with 1 equiv of 1-Mecyt to give the cationic complexes $[M(dmba)(L')(1\text{-Mecyt})]ClO_4$ (**5**−**7**) (Scheme 1). Complexes **5**−**7** are white, air-stable solids that decompose on heating above 239 °C. Their acetone solutions show conductance values corresponding to 1:1 electrolytes.[9] The ^{1}H NMR spectra of complexes **5**−**7** show that both the *N*-methyl and the CH_2 groups of the dmba are diastereotopic, two separate signals being observed for the former and an AB quartet for the latter (some broadening being observed for complexes **5** and **7**). Therefore, there is no plane of symmetry in the palladium coordination plane. In complexes **5** and **6** the PPh_3-trans-to-NMe_2 ligand arrangement in the starting products[22,23] is preserved after chlorine abstraction and 1-Mecyt coordination, as can be inferred from the small but significant coupling constants $^4J_{P-H}$ (ranging from 2.4 to 3.8 Hz) of the NMe_2 and CH_2N protons with the phosphorus atom[24,25] in complex **6**. In complexes **5**−**7** the H(5) and H(6) resonances of 1-Mecyt ligand are also shifted downfield due to the metal binding. Two NH resonances are observed for the coordinated 1-Mecyt ligand in complex **7**, which are also strongly shifted downfield relative to the free base.

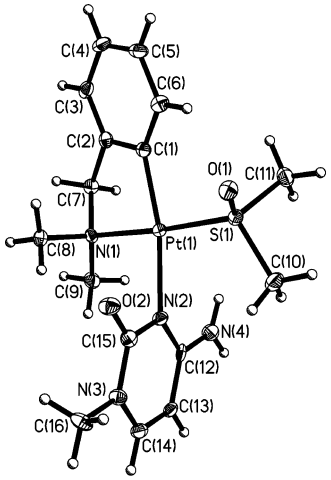

Figure 3. ORTEP of complex **7** showing the atom-numbering scheme. Displacement ellipsoids are drawn at the 50% probability level.

Table 3. Selected Bond Lengths and Angles for Complex **7**

bond lengths, Å		bond angles, deg	
Pt(1)−C(1)	2.015(3)	C(1)−Pt(1)−N(1)	81.89(13)
Pt(1)−N(1)	2.105(3)	C(1)−Pt(1)−N(2)	169.30(12)
Pt(1)−N(2)	2.142(3)	N(1)−Pt(1)−N(2)	90.60(11)
Pt(1)−S(1)	2.2064(9)	C(1)−Pt(1)−S(1)	94.02(10)
		N(1)−Pt(1)−S(1)	175.87(8)
		N(2)−Pt(1)−S(1)	93.53(8)

Crystal Structure of 7. A drawing of the cationic complex of **7** is shown in Figure 3 with selected bond lengths and angles listed in Table 3. The platinum atom is located in a slightly distorted square-planar environment, surrounded by the C and N atoms of the cyclometalated dmba ligand (with a *C*,*N*-bite angle of 81.89(13)°), the DMSO ligand positioned trans to the NMe_2 group, and the 1-Mecyt ligand trans to the aromatic ring. The cyclometalated ring is puckered with the nitrogen atom significantly out of the plane defined by

(19) Krumm, M.; Mutikainen, I.; Lippert, B. *Inorg. Chem.* **1991**, *30*, 884.
(20) Cosar, S.; Janik, M. B. L.; Flock, M.; Freisinger, E.; Farkas, E.; Lippert, B. *J. Chem. Soc., Dalton Trans.* **1999**, 2329.
(21) Navarro, J. A. R.; Lippert, B. *Coord. Chem. Rev.* **2001**, *222*, 219 and references therein.
(22) Deeming, A. J.; Rothwell, I. P.; Hursthouse, M. B.; New, L. *J. Chem. Soc., Dalton Trans.* **1978**, 1490.
(23) Meijer, M. D.; Kleij, A. W.; Williams, B. S.; Ellis, D.; Lutz, M.; Spek, A. L.; van Klink, G. P. M.; van Koten G. *Organometallics* **2002**, *21*, 264.
(24) Braunstein, P.; Matt, D.; Dusausoy, Y.; Fischer, J.; Mitschler, A.; Ricard, L. *J. Am. Chem. Soc.* **1981**, *103*, 5115.
(25) Falvello, L. R.; Fernández, S.; Navarro, R.; Urriolabeitia, E. P. *Inorg. Chem.* **1997**, *36*, 1136.

Table 4. Hydrogen Bonds for Complex 7[a]

D−H···A	*d*(D−H), Å	*d*(H···A), Å	*d*(D···A), Å	<(DHA), deg
N(4)−H(0A)···O(90)#1	0.88(3)	2.10(3)	2.949(4)	161(4)
N(4)−H(0B)···O(6)#1	0.88(3)	2.45(4)	3.107(5)	132(4)
C(14)−H(14)···O(1)#1	0.95	2.44	3.267(4)	145.8
C(16)−H(16A)···O(1)#1	0.98	2.35	3.280(4)	157.8
C(11)−H(11B)···O(6)#1	0.98	2.23	3.190(5)	164.8
C(3)−H(3)···O(6)#2	0.95	2.49	3.283(5)	140.6
C(92)−H(92B)···O(4)#3	0.98	2.57	3.540(6)	169.7
C(10)−H(10C)···O(3)#4	0.98	2.53	3.477(5)	161.7
C(92)−H(92A)···O(1)#5	0.98	2.41	3.231(5)	141.1

[a] Symmetry transformations used to generate equivalent atoms: #1 x, $-y+1/2$, $z-1/2$; #2 $-x+1$, $y-1/2$, $-z+3/2$; #3 x, $-y+3/2$, $z-1/2$; #4 $-x$, $y-1/2$, $-z+1/2$; #5 $-x$, $y+1/2$, $-z+1/2$.

the platinum and carbon atoms, a feature which is quite commonly observed in cyclometalated dmba complexes. The Pt−C(1) (dmba) and Pt−N(1) (dmba) distances are similar to those found in other Pt(dmba) complexes.[23] The 1-Mecyt plane is almost perpendicular to the coordination plane (dihedral angle between the planes = 88.4°). The Pt−N(1-Mecyt) bond distance, 2.142(3) Å, is longer than the values of 2.031(6) and 2.040(6) Å found in the cation *cis*-$[(NH_3)_2$-Pt(1-Mecyt)$_2]^{2+}$ [18] or 2.056(8) Å found in [(trpy)Pt(1-Mecyt)]$^{2+}$.[20] In the crystal a rather complex three-dimensional macromolecular network structure is observed built up by extensive hydrogen bonding which involves the 1-Mecyt ligand, the perchlorate anion, the coordinated DMSO, and the acetone molecule of crystallization (Table 4).

Complexes *cis*-[M(C$_6$F$_5$)$_2$(1-Mecyt)$_2$]. The complexes *cis*-$[NBu_4]_2[Pd_2(C_6F_5)_4(\mu\text{-Cl})_2]$[26] and *cis*-$[Pt(C_6F_5)_2(THF)_2]$[27] are good precursors for the synthesis of complexes **8** and **9**, respectively (Scheme 3). The reactions take place without isomerization, and the reaction products are the cis isomers. Their IR spectra show the characteristic absorptions of the C_6F_5 group (1630 m, 1490 vs, 1050 s, and 950 vs cm^{-1})[11] and a split band at ca. 800 cm^{-1} assigned to the *cis*-M$(C_6F_5)_2$ moiety.[12,13] The ^{19}F NMR spectra of **8** and **9** show the expected three signals for two equivalent C_6F_5 rings with relative intensities of $4F_o$:$2F_p$:$4F_m$. The broad resonance observed at room temperature for the ortho fluorine atoms suggests a hindered rotation of the C_6F_5 ring around the M−C bond. The ^{1}H NMR spectra of complexes **8** and **9** consist of five resonances with relative intensities of 2:2:2:2:6; two NH resonances are observed for the coordinated 1-Mecyt ligands and a unique set of resonances for the H(5), H(6), and Me protons, indicating the presence of only one type of 1-Mecyt group.

Crystal Structure of 8. Figure 4 shows the X-ray structure of complex **8** with selected bond lengths and angles listed in Table 5. The crystal structure of compound **8** shows two independent molecules in the asymmetric unit with the palladium atoms in slightly distorted square-planar geometries. The angles between the two C_6F_5 rings are 85.47(9)° and 86.24(9)°, and the angles between the two 1-Mecyt ligands are 88.14(7)° and 90.05(7)°. The two coordinated

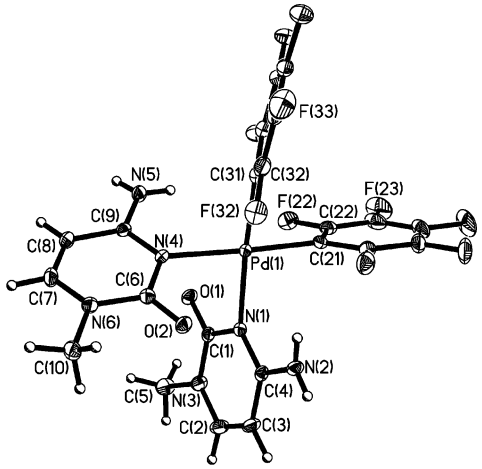

Figure 4. ORTEP of complex **8** showing the atom-numbering scheme. Displacement ellipsoids are drawn at the 50% probability level.

Scheme 3

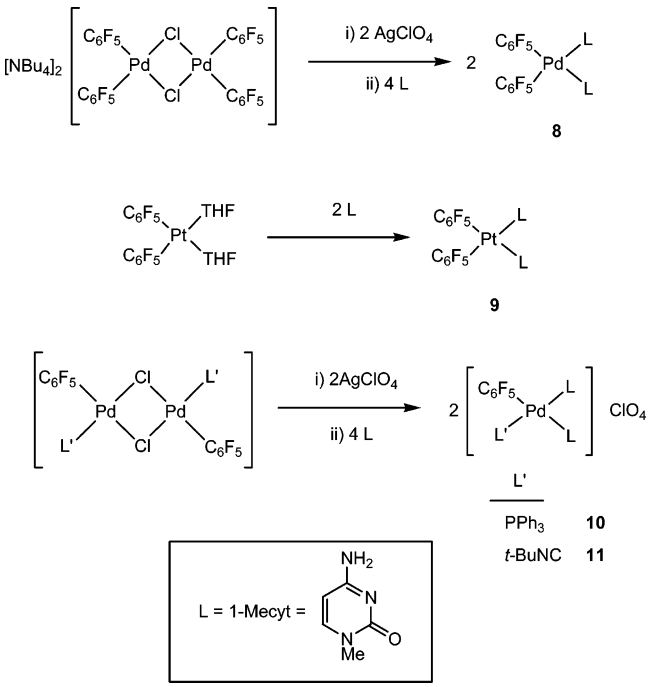

Table 5. Selected Bond Lengths and Angles for Complex **8**

	bond lengths, Å		bond angles, deg	
molecule 1	Pd(1)−C(21)	1.998(2)	C(21)−Pd(1)−C(31)	85.47(9)
	Pd(1)−C(31)	2.005(2)	C(21)−Pd(1)−N(4)	175.97(8)
	Pd(1)−N(4)	2.1111(18)	C(31)−Pd(1)−N(4)	93.97(8)
	Pd(1)−N(1)	2.1187(18)	C(21)−Pd(1)−N(1)	92.76(8)
			C(31)−Pd(1)−N(1)	174.68(8)
			N(4)−Pd(1)−N(1)	88.14(7)
molecule 2	Pd(2)−C(51)	2.002(2)	C(51)−Pd(2)−C(41)	86.24(9)
	Pd(2)−C(41)	2.003(2)	C(51)−Pd(2)−N(7)	173.39(8)
	Pd(2)−N(7)	2.1169(18)	C(41)−Pd(2)−N(7)	92.39(8)
	Pd(2)−N(10)	2.1171(19)	C(51)−Pd(2)−N(10)	91.87(8)
			C(41)−Pd(2)−N(10)	174.61(8)
			N(7)−Pd(2)−N(10)	90.05(7)

1-Mecyt ligands are arranged in a head-to-tail fashion such the complex possesses approximate C_2 molecular symmetry as observed previously in *cis*-$[Pt(NH_3)_2(1\text{-Mecyt})_2]$.[18] There is a relatively short intramolecular contact N2···O2 (3.071 Å). The other contacts N···O are longer (3.162, 3.243, and 3.420 Å). The Pd−N(1-Mecyt) bond distances (Pd(1)−N(4)

(26) Usón, R.; Forniés, J.; Martínez, F.; Tomás, M. *J. Chem. Soc., Dalton Trans.* **1980**, *888*.
(27) Usón, R.; Forniés, J.; Tomás, M.; Menjón, B. *Organometallics* **1985**, *4*, 1912.

Table 6. Hydrogen Bonds for Complex **8**[a]

D−H···A	*d*(D−H), Å	*d*(H···A), Å	*d*(D···A), Å	<(DHA), deg
N(2)−H(0B)···O(2)#1	0.80(3)	2.09(3)	2.861(3)	162(3)
N(5)−H(50A)···O(4)#2	0.85(3)	2.09(3)	2.895(3)	157(3)
N(8)−H(80A)···O(1)#3	0.82(3)	1.96(3)	2.776(3)	172(3)
N(11)−H(11A)···O(3)#4	0.83(3)	2.03(3)	2.821(3)	160(3)

[a] Symmetry transformations used to generate equivalent atoms: #1 $-x+1, -y, -z+2$; #2 $x, y-1, z$; #3 $x, y+1, z$; #4 $-x+2, -y+1, -z+1$.

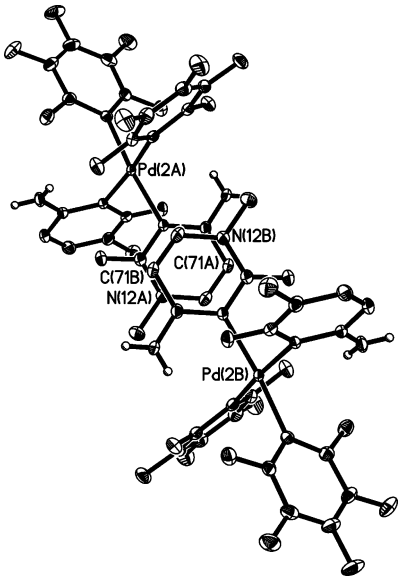

Figure 5. $\pi-\pi$ Interactions in complex **8**.

= 2.1111(18) Å and Pd(1)−N(1) = 2.1187(18) Å) are longer than those observed in complexes **1**, *trans*-$[Pd(NH_3)_2(1\text{-Mecyt})_2]^{2+}$, and $[Pd(1\text{-Mecyt})_4]^{2+}$,[19] although similar to the values found in *cis*-$[Pd(C_6F_5)_2(NH_3)_2]$, *cis*-$[Pd(C_6F_5)_2(NHCMe_2)_2]$,[28] and *cis*-$[Pd(C_6F_5)_2\{NHC(OMe)Me\}_2]$.[29] The planes of the cytosine rings are roughly at right angles to the metal coordination plane with dihedral angles of 72.4° (N1) and 70.8° (N4) in molecule 1 and 72.9° (N7) and 69.1° (N10) in molecule 2. The two 1-Mecyt rings are nearly perpendicular with dihedral angles of 69.1° in molecule 1 and 72.9° in molecule 2. In the crystal there is intermolecular hydrogen bonding (N−H···O) forming infinite chains along the *y* axis (Table 6). There are also intermolecular $\pi-\pi$ interactions between pyrimidine rings of adjacent chains (N(12) of a nucleobase ring of molecules of type 2 with C(71) of another ring of molecules of type 2 of different chain = 3.742 Å; N(3) and C(3) = 3.687 Å and N(1) and C(2) = 3.778 Å of molecules of type 1) (Figure 5). This type of intermolecular stacking interaction has been previously observed in *trans*-$[Pt(NH_3)Cl_2(1\text{-Mecyt})]\cdot 1/2H_2O$.[30]

Complexes *cis*-$[Pd(C_6F_5)(L')(1\text{-Mecyt})_2]ClO_4$. The reaction of $[\{Pd(C_6F_5)(L')(\mu\text{-Cl})\}_2]$ ($L' = PPh_3$,[31] *t*-BuNC[32]) with $AgClO_4$ (1:2 molar ratio) in acetone followed by addition of 2 equiv of 1-Mecyt gives the cationic complexes $[Pd(C_6F_5)(L')(1\text{-Mecyt})_2]ClO_4$ (**10** and **11**) (Scheme 3). In acetone solution complexes **10** and **11** behave as 1:1 electrolytes.[9] The IR spectra of these complexes show an absorption located at 790 cm^{-1} that is observed as a single band for the so-called X-sensitive mode,[12] as expected from the presence of only one C_6F_5 group in the coordination sphere of the palladium atom. The IR spectrum of complex **11** also shows an absorption assigned to ν(CN) of the *t*-BuNC group[33−35] at ca. 2235 cm^{-1}. The ^{19}F NMR spectra of complexes **10** and **11** at room temperature show a unique set of sharp resonances indicating the presence of only one type of C_6F_5 group. The ^1H NMR spectra of complexes **10** and **11** show 10 resonances for the coordinated 1-Mecyt ligands with two distinct sets of resonances for the H(5), H(6), and Me protons, indicating the presence of two types of 1-Mecyt groups, one trans to C_6F_5 and the other trans to L′ (L′ = PPh_3 or *t*-BuNC). The ^1H NMR spectrum of complex **11** shows also a singlet resonance for the *t*-BuNC group at δ 1.43 ppm.

The ^{31}P MNR spectrum of complex **10** shows a unique resonance for the phosphine ligand at δ 23.8 ppm.

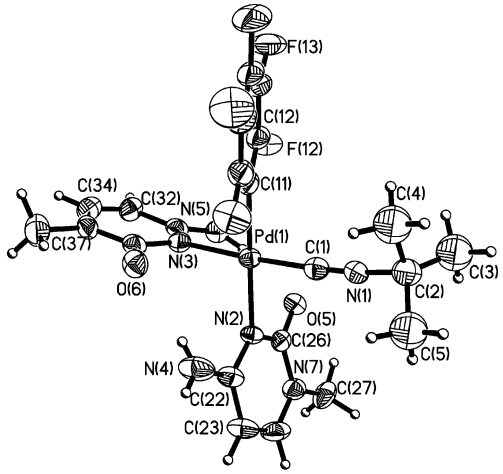

Figure 6. ORTEP of complex **11** showing the atom-numbering scheme. Displacement ellipsoids are drawn at the 50% probability level.

Table 7. Selected Bond Lengths and Angles for Complex **11**

bond lengths, Å		bond angles, deg	
Pd(1)−C(1)	1.922(5)	C(1)−Pd(1)−C(11)	85.19(18)
Pd(1)−C(11)	2.010(4)	C(1)−Pd(1)−N(3)	174.61(16)
Pd(1)−N(3)	2.064(4)	C(11)−Pd(1)−N(3)	90.04(16)
Pd(1)−N(2)	2.092(3)	C(1)−Pd(1)−N(2)	92.27(16)
		C(11)−Pd(1)−N(2)	176.37(16)
		N(3)−Pd(1)−N(2)	92.37(13)

Crystal Structure of 11. Figure 6 shows the X-ray structure of complex **11** with selected bond lengths and angles listed in Table 7. The palladium atom exhibits a distorted square-planar geometry. The angle between the two 1-Mecyt ligands is 92.37(13)°. The two coordinated 1-Mecyt ligands are arranged in a head-to-tail fashion as shown in

(28) Ruiz, J.; Rodríguez, V.; Cutillas, N.; López, G.; Pérez, J. *Organometallics* **2002**, *21*, 4912.
(29) Ruiz, J.; Cutillas, N.; Rodríguez, V.; Sampedro, J.; López, G.; Chaloner, P. A.; Hitchcock, P. B. *J. Chem. Soc., Dalton Trans.* **1999**, 2939.
(30) Lippert, B.; Lock, C. J. L.; Speranzini, R. A. *Inorg. Chem.* **1981**, *20*, 808.
(31) Usón, R.; Forniés, J.; Navarro, R.; García, M. P. *Inorg. Chim. Acta* **1979**, *33*, 69.
(32) Usón, R.; Forniés, J.; Espinet, P.; Lalinde, E. *J. Organomet. Chem.* **1983**, *254*, 371.

Table 8. Hydrogen Bonds for Complex **11**

D−H···A	*d*(D−H), Å	*d*(H···A), Å	*d*(D···A), Å	<(DHA), deg
N(4)−H(40B)···O(6)	0.75(4)	2.21(4)	2.957(6)	174(7)
N(5)−H(50A)···O(5)	0.84(3)	2.05(3)	2.871(5)	168(5)

complex **8**. Two relatively short intramolecular contacts N5···O5 (2.871(5) Å) and N4···O6 (2.957(6) Å) are observed, which suggests a significant extra stabilization of this arrangement due to intramolecular H bonds (Table 8). The Pd−N(1-Mecyt) bond distances (Pd(1)−N(3) = 2.064(4) Å and Pd(1)−N(2) = 2.092(3) Å) are shorter than those observed in complex **8**. The planes of the cytosine rings are roughly at right angles to the metal coordination plane with dihedral angles of 93.0° (N2) and 81.5° (N3). The two 1-Mecyt rings are nearly perpendicular with dihedral angles of 79.7°. There are also intermolecular $\pi-\pi$ interactions between C_6F_5 rings.[36,37] The planes of both rings make an angle of 2.8° with an interplanar distance of 3.43 Å, a center-to-center distance of 4.15 Å, and a deviation of the center-center line of the perpendicular of the plane of 35°.

Biological Assays. *Circular Dichroism Spectroscopy.* The circular dichroism (CD) spectra of Calf thymus DNA alone and incubated with 1-Mecyt and its palladium(II) and platinum(II) compounds at 37 °C for 24 h with several molar ratios were recorded.

The free ligand 1-Mecyt did not significantly modify either the ellipticity of the bands or their position. In contrast, the changes in ellipticity and wavelength caused by the new complexes are significant (Table 9). All complexes, except **7**, decreased the ellipticity of the positive and negative band with increasing values of r_i. An upshift in λ_{max} is also observed. This effect is more important for the palladium than the platinum complexes. These modifications are probably due to a B→C transformation with increasing winding of the DNA helix.[38−42] Complex **7** increased the ellipticity for $r_i = 0.1$ and 0.3 and decreased for $r_i = 0.5$.

Gel Electrophoresis of Compound-pB*R*322 Complexes. The influence of the compounds on the tertiary structure of DNA was determined by their ability to modify the electrophoretic mobility of the covalently closed circular (ccc) and open (oc) forms of pB*R*322 plasmid DNA. The complexes and the 1-Mecyt ligand were incubated at the molar ratio $r_i = 0.50$ with pB*R*322 plasmid DNA at 37 ° C for 24 h. Representative gels obtained for the Pd and Pt complexes **1**−**11** are shown in Figure 7. The behavior of the gel electrophoretic mobility of both forms, ccc and oc, of pB*R*322 plasmid and DNA:cisplatin adducts is consistent with previous reports.[43] No changes were observed in sample incubated with the free ligand 1-Mecyt. When pB*R*322 was incubated with palladium compounds **1** (lane 3) and **10** (lane 12), a retard in the mobility of the ccc form was observed. When pB*R*322 was incubated with compounds **2**, **3**, **5**, **6,** and **8,** a single footprinting for both forms, ccc and oc, coalescent form, was observed.

The behavior observed for the electrophoretic mobility for the palladium and platinum complexes indicates that some conformational change occurred. This means that the degree of superhelicity of the DNA molecules has been altered. In contrast, the free ligand 1-Mecyt does not seem to modify the tertiary structure of DNA.

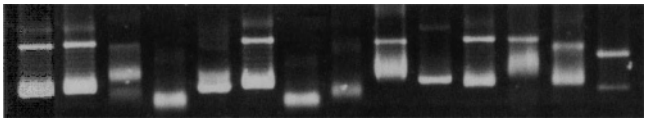

Figure 7. Modification of the gel electrophoretic mobility of pB*R*322 plasmid incubated with 1-Mecyt and its palladium and platinum compounds. Lane 1 shows pB*R*; lane 2, 1-Mecyt; lane 3, complex **1**; lane 4, complex **2**; lane 5, complex **3**; lane 6, complex **4**; lane 7, complex **5**; lane 8, complex **6**; lane 9, complex **7**; lane 10, complex **8**; lane 11, complex **9**; lane 12, complex **10**; lane 13, complex **11**; lane 14, complex *cisplatin*.

Table 9. CD Spectral Data for DNA for Different r_i (molar ratio)

	r_i	λ_{max} (nm)	θ_{max} (deg·cm^2·dmol^{-1})	λ_{min} (nm)	θ_{min} (deg·cm^2·dmol^{-1})
DNA		274.6	5.01×10^3	245.8	-5.86×10^3
1	0.1	279.6	4.00×10^3	245.8	-4.82×10^3
	0.3	280.8	2.33×10^3	246.4	-3.29×10^3
	0.5	282.6	1.54×10^3	247.4	-3.82×10^3
2	0.1	279.8	3.98×10^3	245.8	-4.82×10^3
	0.3	280.8	2.34×10^3	246.6	-3.29×10^3
	0.5	282.6	1.54×10^3	247.4	-3.83×10^3
3	0.1	280.2	4.38×10^3	246.4	-5.40×10^3
	0.3	282.6	3.65×10^3	248.4	-4.63×10^3
	0.5	284.2	2.75×10^3	249.2	-4.56×10^3
4	0.1	274.0	4.46×10^3	245.4	-5.06×10^3
	0.3	277.8	3.44×10^3	243.6	-4.31×10^3
	0.5	281.6	1.87×10^3	247.0	-3.73×10^3
5	0.1	279.0	4.19×10^3	247.2	-5.16×10^3
	0.3	281.8	2.87×10^3	249.0	-4.60×10^3
	0.5	282.6	1.54×10^3	247.4	-3.83×10^3
6	0.1	279.0	4.05×10^3	245.8	-5.36×10^3
	0.3	281.0	3.13×10^3	247.0	-4.50×10^3
	0.5	282.2	2.17×10^3	246.2	-4.15×10^3
7	0.1	278.4	4.83×10^3	246.8	-5.65×10^3
	0.3	278.8	5.15×10^3	247.8	-5.33×10^3
	0.5	281.6	3.89×10^3	246.2	-4.29×10^3
8	0.1	278.6	3.82×10^3	244.4	-5.28×10^3
	0.3	281.0	1.45×10^3	247.4	-2.19×10^3
	0.5	280.4	1.33×10^3	246.4	-1.84×10^3
9	0.1	279.2	4.05×10^3	245.8	-5.22×10^3
	0.3	279.2	3.83×10^3	246.0	-5.15×10^3
	0.5	280.0	3.45×10^3	246.0	-4.88×10^3
10	0.1	279.8	3.98×10^3	245.8	-4.82×10^3
	0.3	280.8	2.33×10^3	246.4	-3.29×10^3
	0.5	226.2	1.79×10^3	247.2	-1.97×10^3
11	0.1	279.6	4.01×10^3	246.0	-4.93×10^3
	0.3	280.6	2.86×10^3	245.6	-4.00×10^3
	0.5	282.2	1.68×10^3	243.6	-2.17×10^3

(33) Ruiz, J.; Rodríguez, V.; Cutillas, N.; Florenciano, F.; Pérez, J.; López, G. *Inorg. Chem. Commun.* **2001**, *4*, 23.
(34) Ruiz, J.; Martínez, M. T.; Vicente, C.; García, G.; López, G.; Chaloner, P. A.; Hitchcock, P. B. *Organometallics* **1993**, *12*, 1594.
(35) Ruiz, J.; López, J. F. J.; Rodríguez, V.; Pérez, J.; Ramírez de Arellano, M. C.; López, G. *J. Chem. Soc., Dalton Trans.* **2001**, 2683.
(36) Collings, J. C.; Roscoe, K. P.; Thomas, R. L.; Batsanov, A. S.; Stimson, L. M.; Howard, J. A. K.; Marder, T. B. *New J. Chem.* **2001**, *25*, 1410.
(37) Vangala, V. R.; Nangia, A.; Lynch, V. M. *Chem. Commun.* **2002**, 1304.
(38) Macquet, J. P.; Butour, J. L. *Biochimie* **1978**, *60*, 901.
(39) Brabec, V.; Kleinwächter, V.; Butour, J.; Johnson, M. P. *Biophys. Chem.* **1990**, *35*, 129.
(40) Marchan, V.; Moreno, V.; Pedroso, E.; Grandas, A. *Chem. Eur. J.* **2002**, *7*, 808.
(41) Zaludová, R.; Zakouská, A.; Kaspárová, J.; Balcarová, Z.; Kleinwächter, V.; Vrána, O.; Farrel, N.; Brabec, V. *Eur. J. Biochem.* **1997**, *246*, 508.
(42) Pérez-Cabré, M.; Cervantes, G.; Moreno, V.; Prieto, M. J.; Pérez, J. M.; Font-Bardia, M.; Solans, X. *J. Inorg. Biochem.* **2004**, *98*, 510.
(43) Ushay, H. M.; Tullius, T. D.; Lippard, S. J. *Biochemistry* **1981**, *20*, 3744.

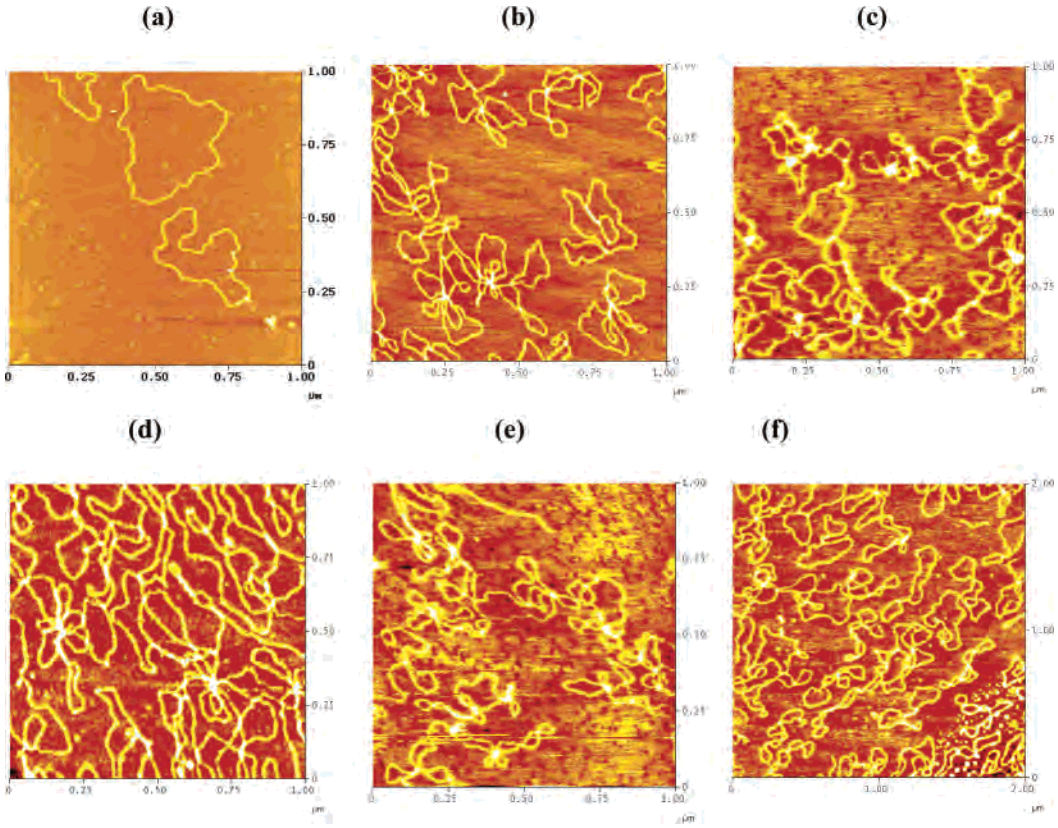

Figure 8. TMAFM image corresponding to pB*R*322 (a), pB*R*−cisplatin (b), pB*R*−complex **1** (c), pB*R*−complex **2** (d), pB*R*−complex **3** (e), and pB*R*−complex **4** (f).

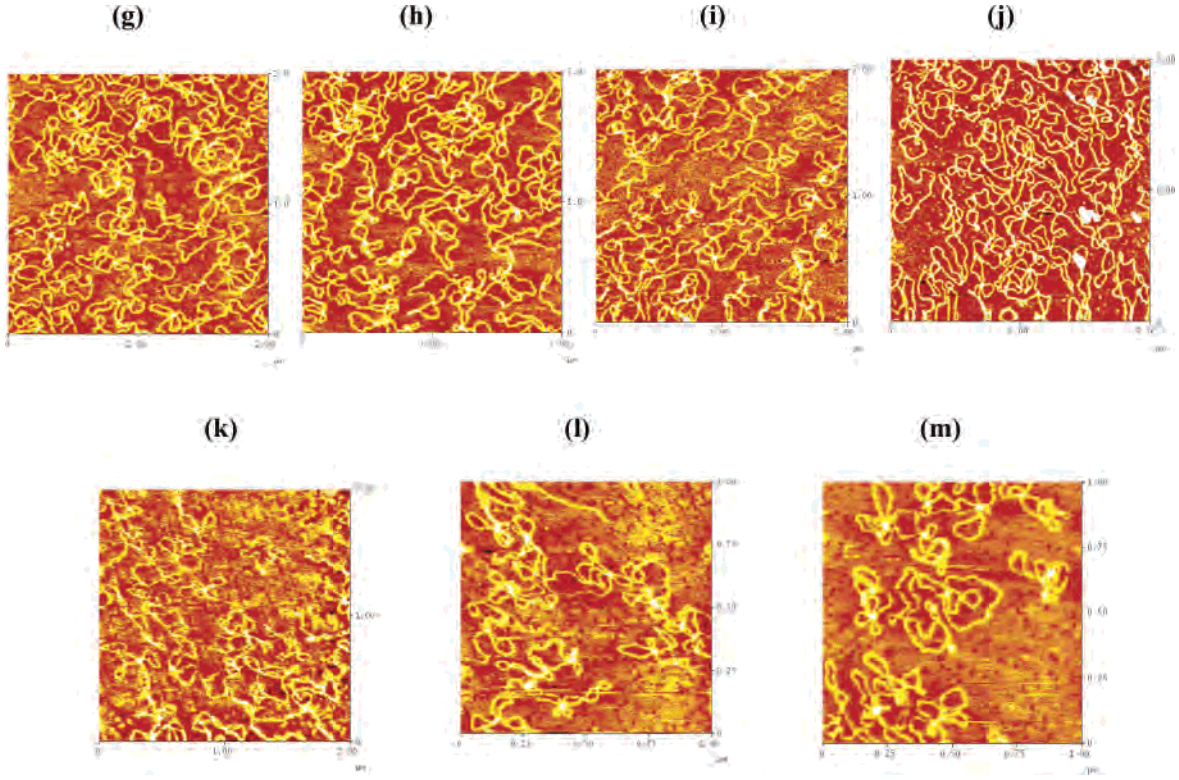

Figure 9. TMAFM image corresponding to pB*R*−complex **5** (g), pB*R*−complex **6** (h), pB*R*−complex **7** (i), pB*R*−complex **8** (j), pB*R*−complex **9** (k), pB*R*−complex **10** (l), and pB*R*−complex **11** (m).

AFM Study of Compound-pB*R*322 Complexes. In Figures 8 and 9 the images corresponding to the modifications caused by the Pd(II) and Pt(II) complexes on pB*R*322 plasmid DNA are shown. In all cases the complexes seem to modify the morphology of the pB*R*322 DNA in similar mode as cisplatin does.[44−47] In the AFM images the same

Table 10. IC_{50} (μM) for Cisplatin and Complexes **1**−**11** for the Tumor Cell Line HL-60

complex	24 h	72 h
cisplatin	15.61	2.15
1	10.80	11.48
2	124.30	104.90
3	6.24	5.27
4	10.89	10.48
5	3.01	2.06
6	3.24	2.98
7	1.36	1.08
8	11.32	11.67
9	1.65	1.42
10	4.71	5.37
11	7.05	6.13

type of effect is observed for palladium or platinum complexes. The metal complexes attached to DNA cause kinks and cross-linking in the plasmid forms.

Cytotoxicity Studies. The in vitro growth inhibitory effect of complexes **1**−**11** and cisplatin was evaluated in HL-60 human tumor cell line. As listed in Table 10, at a short incubation time (24 h) all of the new complexes (except complex **2**) were more active than cisplatin. In fact, at a 24 h incubation time complexes **7** and **9** were about 10-fold more active than cisplatin toward HL60 cells. After 72 h of incubation time complexes **7** and **9** were also 2-fold more active than cisplatin, while the rest of complexes were less active than cisplatin.

In Vitro Apoptosis Assay. The most common and well-defined form of programmed cell death is apoptosis, which is a physiological cell suicide program that is essential for the maintenance of tissue homeostasis in multicellular organisms. In contrast to the self-contained nature of apoptotic cell death, necrosis is a messy, unregulated process of traumatic cell destruction, which is followed by the release of intracellular components. During the past decade cell biology as well as oncology research has focused on this latter process of programmed cell death or apoptosis. It is anticipated that an understanding of the basic mechanisms that underlie apoptosis will offer potential new targets for therapeutic treatment of diseases.[48]

The type of cell death induced by the new complexes was investigated by Annexin V/PI apoptosis assay in a flow cytometer. The results obtained for the different complexes at 24 h of incubation time were compared with those for cisplatin. With all drugs apoptosis was observed, and the percentages are presented in Table 11. Exposure of cells to cisplatin and complexes **1**−**8** and **11** resulted in a significant induction of apoptosis (30−45% of apoptotic cells) compared with that produced by complexes **9** and **10** (8−15% of apoptotic cells). However, an additional population of cells appeared to be dying by necrosis or late apoptosis when HL60 cells were exposed to complexes **1**−**11**.

Table 11. Percentages of Vital Cells, Apoptotic Cells, Dead Cells, and Damaged Cells after Treatment of a HL-60 Cell Population with Cisplatin and Complexes **1**−**11** for 24 h

treatment (IC_{50} 24 h, mM)	% vital cells (R1)	% apoptotic cells (R2)	% dead cells (R3)	% damaged cells (R4)
control	89.65	2.81	6.79	0.75
cisplatin (15.6)	54.89	37.57	5.17	2.37
1 (10.80)	33.75	40.42	20.68	5.16
2 (124.3)	44.46	36.34	16.77	2.43
3 (6.4)	35.18	39.04	21.47	4.31
4 (10.89)	44.84	30.39	19.30	5.47
5 (3.02)	54.67	21.09	19.43	4.81
6 (3.24)	41.25	36.09	16.21	6.45
7 (1.36)	40.22	38.80	17.42	3.56
8 (11.32)	44.30	31.20	17.94	6.56
9 (1.66)	81.85	7.99	8.99	1.27
10 (4.71)	74.32	14.84	10.32	0.52
11 (7.05)	34.76	46.63	17.12	1.49

Conclusions

New palladium and platinum organometallic complexes derived from the 2-(dimethylaminomethyl)phenyl (dmba) and pentafluorphenyl groups with the model nucleobase 1-methylcytosine have been prepared. The crystal structures of [Pd(bpzm*)(C_6F_5)(1-Mecyt)]ClO_4,[Pt(dmba)(DMSO)(1-Mecyt)]ClO_4, *cis*-[Pd(C_6F_5)$_2$(1-Mecyt)$_2$], and *cis*-[Pd(*t*-BuNC)(C_6F_5)(1-Mecyt)$_2$]ClO_4 have been established by X-ray diffraction. There is extensive hydrogen bonding (N−H···O, C−H···F, or C−H···O) in all compounds. There are also intermolecular $\pi-\pi$ interactions between pyrimidine rings of adjacent chains in [Pd(C_6F_5)$_2$(1-Mecyt)$_2$]. DNA adduct formation of the new complexes synthesized was followed by circular dichroism and electrophoretic mobility. Atomic force microscopy images of the modifications caused by the complexes on plasmid DNA pB*R*322 were also obtained. In all cases the complexes seem to modify the morphology of the pB*R*322 DNA in similar mode to that of cisplatin. Values of IC_{50} were also calculated for the new complexes against the tumor cell line HL-60. At a short incubation time (24 h) almost all the new complexes were more active than cisplatin. It was demonstrated by flow cytometry that the majority of the cell death observed in cytotoxic assays is by apoptosis.

Experimental Section

Instrumental Measurements. The C, H, and N analyses were performed with a Carlo Erba model EA 1108 microanalyzer. Decomposition temperatures were determined with a Mettler TG-50 thermobalance at a heating rate of 5 °C min^{-1} and the solid samples under nitrogen flow (100 mL min^{-1}). Molar conductivities were measured in acetone solution ($c \approx 5 \times 10^{-4}$ mol L^{-1}) with a Crison 525 conductimeter. The ^{1}H, ^{13}C, ^{31}P, and ^{19}F NMR spectra were recorded on a Bruker AC 200E or Bruker AC 300E spectrometer using $SiMe_4$, H_3PO_4, and $CFCl_3$ as standards. The ^{195}Pt NMR spectra were recorded on a Bruker AV 400 spectrometer using $Na_2[PtCl_6]$ as standard. Infrared spectra were recorded on a Perkin-Elmer 1430 spectrophotometer using Nujol mulls between polyethylene sheets. Solvents were dried by the usual methods.

Materials. The starting complexes [(N−N)Pd(C_6F_5)Cl] (N−N = bpzm*, bpzm,[14] tmeda, and bpy),[49] [(*o*-$C_6H_4CH_2NMe_2$)PdCl(PPh$_3$)],[22] [(*o*-$C_6H_4CH_2NMe_2$)PtCl(L′)] (L′ = PPh$_3$ and DMSO),[23]

(44) Cervantes, G.; Prieto, M. J.; Moreno, V. *Met. Based Drugs* **1997**, *4*, 9.
(45) Onoa, G. B.; Cervantes, G.; Moreno, V.; Prieto, M. J. *Nucleic Acid Res.* **1998**, *26*, 1473.
(46) Cervantes, G.; Marchal, S.; Prieto, M. J.; Pérez, J. M.; González, V. M.; Alonso, C.; Moreno, V. *J. Inorg. Biochem.* **1999**, *77*, 197.
(47) Onoa, G. B.; Moreno, V. *Int. J. Pharm.* **2002**, *245*, 55.
(48) Martin, S. J.; Green, D. R. *Curr. Opin. Oncol.* **1994**, *6*, 616.
(49) Usón, R.; Forniés, J.; Martínez, F. *J. Organomet. Chem.* **1976**, *112*, 105.

cis-$[Pd_2(C_6F_5)_4(\mu\text{-}Cl)_2]^{2-}$,[26] *cis*-$[Pt(C_6F_5)_2(THF)_2]$,[27] and $[\{Pd(C_6F_5)(L')(\mu\text{-}Cl)\}_2]$ ($L' = PPh_3$,[31] *t*-BuNC[32]) were prepared by procedures described elsewhere. 1-Methylcytosine (1-Mecyt) was purchased from Chemogen (Konstanz, Germany). The sodium salt of Calf thymus DNA, EDTA (ethylenediaminetetraacetic acid), and Tris-HCl (tris-(hydroxymethyl)aminomethane hydrochloride) used in the circular dichroism (CD) study were obtained from Sigma (Madrid, Spain), HEPES (*N*-2-hydroxyethyl piperazyne-*N*′-2-ethanesulfonic acid) was obtained from ICN (Madrid), and p*BR*322 plasmid DNA was obtained from Boehringer-Mannheim (Mannheim, Germany).

Warning! Perchlorate salts of metal complexes with organic ligands are potentially explosive. Only small amounts of material should be prepared, and these should be handled with great caution.

Preparation of Complexes [Pd(N−N)(C_6F_5)(1-Mecyt)]ClO_4 [N−N = bpzm* (1), bpzm (2), tmeda (3), bpy (4)]. To a solution of [PdCl(C_6F_5)(N−N)] (0.194 mmol) in acetone (20 mL) was added $AgClO_4$ (40.4 mg, 0.194 mmol). AgCl immediately formed. The resulting suspension was stirred for 30 min and then filtered through a short pad of Celite. To the filtrate was then added 1-methylcytosine (24.3 mg, 0.194 mmol). The solution was stirred for 24 h, and then the solvent was partially evaporated under vacuum and water (for **1** and **2**) or hexane (for **3** and **4**) added to precipitate a white solid, which was collected by filtration and air-dried.

Data for Complex 1. Yield: 75 mg, 55%. Anal. Calcd for $C_{22}H_{23}ClF_5N_7O_5Pd$: C, 37.6; H, 3.3; N, 14.0. Found: C, 37.9; H, 3.1; N, 13.7. Mp: 260 °C dec. Λ_M: 152 S cm^2 mol^{-1}. IR (Nujol, cm^{-1}): ν(NH), 3327, 3230; ν(Pd−C_6F_5), 778. ^{1}H NMR (acetone-d_6): δ(SiMe$_4$) 8.37 (br, 1H, NH_2), 8.19 (br, 1H, NH_2), 7.78 (d, 1H, CH_2, *J* 15 Hz), 7.74 (d, 1H, H6 of 1-Mecyt, *J* 7.2 Hz), 6.91 (d, 1H, CH_2, *J* 15 Hz), 6.09 (s, 1H, H4′), 6.07 (s, 1 H, H4), 6.01 (d, 1H, H5 of 1-Mecyt, *J* 7.2 Hz), 3.33 (s, 3H, Me of 1-Mecyt), 2.60 (s, 3H, Me3′), 2.58 (s, 3H, Me5), 2.16 (s, 3H, Me5′), 1.99 (s, 3 H, Me3). ^{13}C{^{1}H} NMR ($CDCl_3$): δ(SiMe$_4$) 150.4 (C6 of 1-Mecyt), 109.9, 109.5 (C4 or C4′ of bpzm*), 94.5 (C5 of 1-Mecyt), 59.8 (CH_2 of bpzm*), 39.0 (Me of 1-Mecyt), 14.7, 14.0, 12.2, 11.9 (Me of bpzm*). ^{19}F NMR (acetone-d_6): δ($CFCl_3$) −117.1 (d, 2F_o, $J(F_oF_m)$ 22.5 Hz), −161.2 (t, 1F_p, $J(F_mF_p)$ 19.7 Hz), −164.9 (m, 2F_m).

Data for Complex 2. Yield: 80 mg, 57%. Anal. Calcd for $C_{18}H_{15}ClF_5N_7O_5Pd$: C, 33.5; H, 2.3; N, 15.2. Found: C, 33.5; H, 2.2; N, 15.0. Mp: 248 °C dec. Λ_M: 140 S cm^2 mol^{-1}. IR (Nujol, cm^{-1}): ν(NH), 3425; ν(Pd−C_6F_5), 773. ^{1}H NMR (acetone-d_6): δ(SiMe$_4$) 8.29 (m, 2H, H5 + H5′), 8.04 (br, 1H, NH_2), 7.93 (br, 1H, NH_2), 7.78 (d, 1H, H6 of 1-Mecyt, *J* 7.2 Hz), 7.77 (d, 1H, H3 or H3′, *J* 1.8 Hz), 7.40 (d, 1H, H3 or H3′, *J* 2.0 Hz), 7.37 (d, 1H, CH_2, *J* 15.2 Hz), 7.25 (d, 1H, CH_2, *J* 15.2 Hz), 6.52 (m, 2H, H4 + H4′), 5.96 (d, 1H, H5 of 1-Mecyt, *J* 7.2 Hz), 3.46 (s, 3H, Me of 1-Mecyt). ^{19}F NMR (acetone-d_6): δ($CFCl_3$) −118.6 (br, 2F_o), −161.4 (t, 1F_p, *J* (F_mF_p) 18.8 Hz), −164.8 (br, 2F_m).

Data for Complex 3. Yield: 101 mg, 70%. Anal. Calcd for $C_{17}H_{23}ClF_5N_5O_5Pd$: C, 33.2; H, 3.8; N, 11.4. Found: C, 33.5; H, 4.1; N, 11.6. Mp: 237 °C dec. Λ_M: 135 S cm^2 mol^{-1}. IR (Nujol, cm^{-1}): ν(NH), 3416, 3321; ν(Pd−C_6F_5), 773. ^{1}H NMR (acetone-d_6): δ(SiMe$_4$) 8.55 (br, 1H, NH_2), 7.86 (br, 1H, NH_2), 7.65 (d, 1H, H6 of 1-Mecyt, *J* 7.2 Hz), 5.98 (d, 1H, H5 of 1-Mecyt, *J* 7.2 Hz), 3.37 (s, 3H, Me of 1-Mecyt), 3.13 (br, 4H, CH_2), 2.08 (s, 12H, Me).^{19}F NMR (acetone-d_6): δ($CFCl_3$) −117.2 (d, 2F_o, $J(F_oF_m)$ 18.8 Hz), −162.1 (t, 1F_p, $J(F_mF_p)$ 26.4 Hz), −164.7 (m, 2F_m).

Data for Complex 4. Yield: 115 mg, 85%. Anal. Calcd for $C_{21}H_{15}ClF_5N_5O_5Pd$: C, 38.6; H, 2.3; N, 10.7. Found: C, 38.4; H, 2.3; N, 9.8. Mp: 282 °C dec. Λ_M: 132 S cm^2 mol^{-1}. IR (Nujol, cm^{-1}): ν(NH), 3328, 3462; ν(Pd−C_6F_5), 767. ^{1}H NMR (DMSO-d_6): δ(SiMe$_4$) 8.70 (d, 1H, H_α, $J(H_\alpha H_\beta)$ 3.9 Hz), 8.67 (d, 1H, H_δ, $J(H_\delta H_\gamma)$ 4.2 Hz), 8.60 (br, 1H, NH_2), 8.49 (br, 1H, NH_2), 8.36 (m, 2H, H_γ+$H_{\gamma'}$), 8.08 (d, 1H, $H_{\delta'}$, $J(H_{\delta'}H_{\gamma'})$ 4.2 Hz), 7.83 (d, 1H, $H_{\alpha'}$, $J(H_{\alpha'}H_{\beta'})$ 4.9 Hz), 7.76 (d, 1H, H6 of 1-Mecyt, *J* 7.2 Hz), 7.74 (m, 1H, H_β), 7.33 (m, 1H, $H_{\beta'}$), 5.83 (d, 1H, H5 of 1-Mecyt, *J* 7.2 Hz), 3.22 (s, 3H, Me of 1-Mecyt). ^{19}F NMR (DMSO-d_6): δ($CFCl_3$) −115.8 (d, 1F_o, $J(F_oF_m)$ 31.1 Hz), −117.4 (d, 1F_o, $J(F_oF_m)$ 31.1 Hz), −159.2 (t, 1F_p, $J(F_mF_p)$ 22.6 Hz), −161.6 (m, 1F_m), −162.6 (m, 1F_m).

Preparation of Complexes [M(dmba)(PPh_3)(1-Mecyt)]ClO_4 [M = Pd (5), Pt (6)]. To a solution of [M(dmba)(PPh_3)Cl] (0.185 mmol) (M = Pd or Pt) in acetone (20 mL) was added $AgClO_4$ (38.4 mg, 0.185 mmol). AgCl immediately formed. The resulting suspension was stirred for 30 min and then filtered through a short pad of Celite. To the filtrate was then added 1-methylcytosine (23.1 mg, 0.185 mmol). The solution was stirred for 6 h, and then the solvent was partially evaporated under vacuum and water added to precipitate a white solid, which was collected by filtration and air-dried.

Data for Complex 5. Yield: 81 mg, 60%. Anal. Calcd for $C_{32}H_{34}ClN_4O_5PPd$: C, 52.8; H, 4.7; N, 7.7. Found: C, 52.5; H, 4.7; N, 7.5. Mp: 239 °C dec. Λ_M: 165 S cm^2 mol^{-1}. IR (Nujol, cm^{-1}): ν(NH), 3432, 3330. ^{1}H NMR ($CDCl_3$): δ(SiMe$_4$) 7.66−7.30 (m, 17 H, P*Ph*$_3$ + NH_2), 6.97 (d, 1H, C_6H_4, J_{HH} = 7.0 Hz), 6.83 (m, 2H, H6 of 1-Mecyt + C_6H_4), 6.34 (false t, 1 H, C_6H_4, $J_{HH} \cong J_{HH}$ = 7.0 Hz), 6.26 (false t, 1 H, C_6H_4, $J_{HH} \cong J_{HH}$ = 7.0 Hz), 5.76 (d, 1H, H5 of 1-Mecyt, *J* 7.2 Hz), 4.30 (br, 1 H, NCH_2), 3.83 (br, 1 H, NCH_2), 3.03 (s, 3H, Me of 1-Mecyt), 2.70 (br, 3H, N*Me*$_2$), 2.63 (br, 3H, N*Me*$_2$). ^{31}P NMR ($CDCl_3$): δ(H_3PO_4) 43.5 (s).

Data for Complex 6. Yield: 100 mg, 77%. Anal. Calcd for $C_{32}H_{34}ClN_4O_5PPt$: C, 47.1; H, 4.2; N, 6.9. Found: C, 46.9; H, 4.3; N, 6.7; S, 5.6. Mp: 281 °C dec. Λ_M: 110 S cm^2 mol^{-1}. IR (Nujol, cm^{-1}): ν(NH), 3423, 3309. ^{1}H NMR ($CDCl_3$): δ(SiMe$_4$) 7.71−7.37 (m, 17 H, P*Ph*$_3$ + NH_2), 7.09 (d, 1H, C_6H_4, J_{HH} = 7.1 Hz), 6.90 (m, 2 H, H6 of 1-Mecyt + C_6H_4), 6.43 (m, 2 H, C_6H_4), 5.94 (d, 1H, H5 of 1-Mecyt, *J* 7.2 Hz), 4.35 (d, 1 H, NCH_2, J_{HH} = 13.5 Hz), 3.94 (dd, 1 H, NCH_2, J_{HH} = 13.5 Hz, J_{HP} = 3.8 Hz), 3.10 (s, 3H, Me of 1-Mecyt), 2.83 (d, 3H, N*Me* of dmba, J_{HP} = 2.4 Hz), 2.77 (d, 3H, N*Me* of dmba, J_{HP} = 2.7 Hz). ^{13}C{^{1}H} NMR ($CDCl_3$): δ(SiMe$_4$) 148.3 (C6 of 1-Mecyt), 96.8 (C5 of 1-Mecyt), 71.2 (*C*H_2NMe$_2$), 51.0 (N*Me*$_2$), 50.4 (N*Me*$_2$), 39.8 (Me of 1-Mecyt). ^{31}P NMR ($CDCl_3$): δ(H_3PO_4) 20.7 (J_{Pt-P} = 4104 Hz). ^{195}Pt NMR ($CDCl_3$): δ($Na_2[PtCl_6]$) − 3761 (d, J_{Pt-P} = 4104 Hz).

Preparation of Complex [Pt(dmba)(DMSO)(1-Mecyt)]ClO_4 (7). To a solution of [Pt(dmba)(DMSO)Cl] (100 mg, 0.236 mmol) in acetone (20 mL) was added $AgClO_4$ (53.2 mg, 0.236 mmol). AgCl immediately formed. The resulting suspension was stirred for 30 min and then filtered through a short pad of Celite. To the filtrate was then added 1-methylcytosine (29.5 mg, 0.236 mmol). The solution was stirred for 6 h, and then the solvent was partially evaporated under vacuum and methanol added to precipitate a brown solid, which was collected by filtration and air-dried.

Data for Complex 7. Yield: 84 mg, 56%. Anal. Calcd for $C_{16}H_{25}ClN_4O_6SPt$: C, 30.4; H, 4.0; N, 8.9. Found: C, 30.7; H, 4.2; N, 8.5. Mp: 241 °C dec. Λ_M: 130 S cm^2 mol^{-1}. IR (Nujol, cm^{-1}): ν(NH), 3415, 3303. ^{1}H NMR ($CDCl_3$): δ(SiMe$_4$) 7.67 (s, 1H, NH_2), 7.65 (s, 1H, NH_2), 7.56 (d, 1H, H6 of 1-Mecyt, *J* 7.2 Hz), 7.11−6.98 (m, 4 H, C_6H_4), 6.34 (d, 1H, H5 of 1-Mecyt, *J* 7.2 Hz), 4.17 (br, 1 H, NCH_2 dmba), 4.02 (br, 1 H, NCH_2 dmba), 3.49 (s, 3H, Me of 1-Mecyt), 3.39 (brs, 3H, N*Me*$_2$), 3.25 (brs, 3H, N*Me*$_2$), 2.73 (s, 6H, Me of DMSO). ^{195}Pt NMR ($CDCl_3$): δ($Na_2[PtCl_6]$) − 3761 (s).

Preparation of Complex *cis*-[Pd(C_6F_5)$_2$(1-Mecyt)$_2$] (8). To a solution of *cis*-$[NBu_4]_2[Pd_2(C_6F_5)_4(\mu\text{-}Cl)_2]$ (100 mg, 0.070 mmol) in acetone (20 mL) was added $AgClO_4$ (28.9 mg, 0.140 mmol). AgCl immediately formed. The resulting suspension was stirred

Table 12. Crystal Structure Determination Details

	1	7	8	11
formula	$C_{22}H_{23}ClF_5N_7O_5Pd$	$C_{19}H_{31}ClN_4O_7PtS$	$C_{25}H_{20}F_{10}N_6O_3Pd$	$C_{21}H_{23}ClF_5N_7O_6Pd$
fw	702.32	690.08	748.87	706.31
cryst syst	monoclinic	monoclinic	triclinic	orthorhombic
unit cell dimensions				
<ind>*a* (Å)	15.1602(17)	13.6323(6)	9.7297(11)	33.700(2)
<ind>*b* (Å)	22.5242(17)	13.9239(6)	16.7595(19)	12.1319(11)
<ind>*c* (Å)	16.9832(13)	14.2497(6)	18.023(2)	13.9242(11)
<ind>a (deg)	90	90	96.245(2)	90
<ind>b (deg)	110.724(8)	116.498(2)	96.146(2)	90
<ind>*g* (deg)	90	90	104.737(2)	90
unit cell vol (Å^3)	5424.0(8)	2420.66(18)	2797.5(5)	5692.8(8)
temp	173(2)	100(2)	100(2)	173(2)
space group	*P*2(1)/*n*	*P*2(1)/*c*	$P\bar{1}$	Pbcn
Z	8	4	4	8
μ(mm^{-1})	0.865	6.040	0.771	0.827
reflns collected	10 667	26 390	32 634	8453
independent reflns	9514	4932	12 514	5008
R(int)	0.0233	0.0284	0.0217	0.0328
$R1$ [$I > 2\sigma(I)$][a]	0.0333	0.0239	0.0330	0.0401
wR_2 (all data)[b]	0.0766	0.0525	0.0758	0.0997

[a] $R1 = \Sigma||F_o| - |F_c||/\Sigma|F_o|$, $wR2 = [\Sigma[w(F_o^2 - F_c^2)^2]/\Sigma w(F_o^2)^2]^{0.5}$. [b] $w = 1/[\sigma^2(F_o^2) + (aP)^2 + bP]$, where $P = (2F_c^2 + F_o^2)/3$ and a and b are constants set by the program.

for 30 min and then filtered through a short pad of Celite. To the filtrate was then added 1-methylcytosine (38.5 mg, 0.308 mmol). The solution was stirred for 24 h, and then the solvent was partially evaporated under vacuum and hexane added to precipitate a white solid, which was collected by filtration and air-dried.

Data for Complex 8. Yield: 70 mg, 65%. Anal. Calcd for $C_{22}H_{14}F_{10}N_6O_2Pd$: C, 38.3; H, 2.0; N, 12.2. Found: C, 38.4; H, 2.2; N, 12.3. Mp: 232 °C dec. IR (Nujol, cm^{-1}): ν(NH), 3416; ν(Pd−C_6F_5), 784. ^{1}H NMR (acetone-d_6): δ(SiMe$_4$) 8.64 (br, 2H, NH_2), 7.65 (br, 2H, NH_2), 7.58 (d, 2H, H6 of 1-Mecyt, *J* 7.2 Hz), 5.88 (d, 2H, H5 of 1-Mecyt, *J* 7.2 Hz), 3.27 (s, 6H, Me of 1-Mecyt). ^{19}F NMR (acetone-d_6): δ(CFCl$_3$) −114.4 (br, 4F$_o$), −165.6 (t, 2F$_p$, J(F$_m$F$_p$) 19.8 Hz), −167.1 (m, 4F$_m$).

Preparation of Complex *cis*-[Pt(C$_6$F$_5$)$_2$(1-Mecyt)$_2$] (9). To a solution of *cis*-[Pt(C$_6$F$_5$)$_2$(THF)$_2$] (145 mg, 0.215 mmol) in acetone (20 mL) was added 1-methylcytosine (53.8 mg, 0.43 mmol). The solution was stirred for 24 h, and then the solvent was partially evaporated under vacuum and hexane added to precipitate a white solid, which was collected by filtration and air-dried.

Data for Complex 9. Yield: 129 mg, 79%. Anal. Calcd for $C_{22}H_{14}F_{10}N_6O_2Pt$: C, 33.9; H, 1.8; N, 10.8. Found: C, 34.2; H, 1.9; N, 10.6. Mp: 306 °C dec. IR (Nujol, cm^{-1}): ν(NH), 3375, 3197; ν(Pt−C_6F_5), 801. ^{1}H NMR (acetone-d_6): δ(SiMe$_4$) 8.99 (br, 2H, NH_2), 7.66 (br, 2H, NH_2), 7.58 (d, 2H, H6 of 1-Mecyt, *J* 7.2 Hz), 5.92 (d, 2H, H5 of 1-Mecyt, *J* 7.2 Hz), 3.28 (s, 6H, Me of 1-Mecyt). ^{13}C{^{1}H} NMR (CDCl$_3$): δ(SiMe$_4$) 148.8 (C6 of 1-Mecyt), 94.9 (C5 of 1-Mecyt), 38.9 (Me of 1-Mecyt). ^{19}F NMR (acetone-d_6): δ(CFCl$_3$) −118.2 (br, 4F$_o$), −167.0 (t, 2F$_p$, J(F$_m$F$_p$) 19.8 Hz), −168.0 (m, 4F$_m$). ^{195}Pt NMR (CDCl$_3$) at 45 °C: δ(Na$_2$[PtCl$_6$]) − 3636 (t, J_{Pt-Fo} = 480 Hz).

Preparation of Complexes *cis*-[Pd(C$_6$F$_5$)(L′)(1-Mecyt)$_2$]ClO$_4$ [L′ = PPh$_3$ (10), *t*-BuNC (11)]. To a solution of [{Pd(C$_6$F$_5$)(L′)-(μ-Cl)}$_2$] (L′ = PPh$_3$, *t*-BuNC) (0.128 mmol) in acetone (20 mL) was added AgClO$_4$ (52.9 mg, 0.256 mmol). AgCl immediately formed. The resulting suspension was stirred for 30 min and then filtered through a short pad of Celite. To the filtrate was added 1-methylcytosine (63.8 mg, 0.51 mmol). The solution was stirred for 24 h, and then the solvent was partially evaporated under vacuum and hexane added to precipitate a white solid, which was collected by filtration and air-dried.

Data for Complex 10. Yield: 90.4 mg, 70%. Anal. Calcd for $C_{34}H_{29}ClF_5N_6O_6PPd$: C, 46.1; H, 3.3; N, 9.5. Found: C, 45.8; H, 3.2; N, 9.3. Mp: 264 °C dec. Λ_M: 140 S cm^2 mol^{-1}. IR (Nujol, cm^{-1}): ν(NH), 3344; ν(Pd−C_6F_5), 786. ^{1}H NMR (acetone-d_6): δ(SiMe$_4$) 8.60 (br, 1H, NH_2), 8.17 (br, 1H, NH_2), 7.86 (br, 1H, NH_2), 7.72−7.40 (m, 16 H, PPh_3 + NH), 5.95 (d, 1H, H6 of 1-Mecyt, *J* 7.2 Hz), 5.93 (d, 1H, H6 of 1-Mecyt, *J* 7.2 Hz), 5.79 (d, 1H, H5 of 1-Mecyt, *J* 7.2 Hz), 5.77 (d, 1H, H5 of 1-Mecyt, *J* 7.2 Hz), 3.40 (s, 3H, Me of 1-Mecyt), 3.08 (s, 3H, Me of 1-Mecyt). ^{19}F NMR (acetone-d_6): δ(CFCl$_3$) −115.0 (d, 1F$_o$, J(F$_o$F$_m$) 24.5 Hz), −116.3 (d, 1F$_o$, J(F$_o$F$_m$) 28.2 Hz), −162.4 (t, 1F$_p$, J(F$_m$F$_p$) 20.7 Hz), −164.7 (m, 2F$_m$). ^{31}P NMR (acetone-d_6): δ(H$_3$PO$_4$) 23.8 (s).

Data for Complex 11. Yield: 108 mg, 60%. Anal. Calcd for $C_{21}H_{23}ClF_5N_6O_6Pd$: C, 35.7; H, 3.3; N, 13.9. Found: C, 35.6; H, 3.3; N, 13.7. Mp: 293 °C dec. Λ_M: 135 S cm^2 mol^{-1}. IR (Nujol, cm^{-1}): ν(NH), 3366; ν(CN), 2236; ν(Pd−C_6F_5), 776. ^{1}H NMR (acetone-d_6): δ(SiMe$_4$) 8.29 (br, 1H, NH_2), 8.292 (br, 1H, NH_2), 8.97 (br, 1H, NH_2), 7.90 (br, 1H, NH_2), 7.89 (d, 1H, H6 of 1-Mecyt, *J* 7.2 Hz), 7.71 (d, 1H, H6 of 1-Mecyt, *J* 7.2 Hz), 6.15 (d, 1H, H5 of 1-Mecyt, *J* 7.5 Hz), 5.99 (d, 1H, H5 of 1-Mecyt, *J* 7.2 Hz), 3.51 (s, 3H, Me of 1-Mecyt), 3.35 (s, 3H, Me of 1-Mecyt), 1.43 (s, 9 H, *t*-BuNC). ^{19}F NMR (acetone-d_6): δ(CFCl$_3$) −118.3 (d, 2F$_o$, J(F$_o$F$_m$) 20.7 Hz), −161.4 (t, 1F$_p$, J(F$_m$F$_p$) 20.7 Hz), −165.1 (m, 2F$_m$).

X-ray Crystal Structure Analysis. Suitable crystals of **1**, **7**, **8,** and **11** were grown from acetone/hexane. The crystal and molecular structures of the compounds **1**, **7**, **8,** and **11** have been determined by X-ray diffraction studies (Table 12). Crystals were mounted on glass fibers and transferred to the cold gas stream of the diffractometer (**1** and **11** Siemens P4 and the others Bruker Smart APEX). Data were recorded with Mo Kα radiation (λ = 0.71073Å) in ω-scan mode. Absorption correction for compounds **1** and **11** was based on Ψ-scans and for compounds **7** and **8** on multiscans. Structures **1**, **8**, and **11** were solved by the heavy atom method; structure **7** was solved by direct methods and refined anisotropically on F^2.[50] The hydrogens at N were located in the Fourier difference maps and refined freely. Methyl groups were refined using rigid groups, and other hydrogens were refined using a riding method.

Special Features. For compound **1** the perchlorate anion is disordered over two sites, ca. 52:48.

For compound **8** the two acetone molecules are disordered over two sites.

(50) Sheldrick, G. M. *SHELXL-97*; University of Göttingen: Göttingen Germany, 1997.

For compound **11** the *tert*-butyl group is disordered over two sites, ca. 58:42, and the perchlorate is also disordered over two sites, ca. 78:22.

Biological Assays

Formation of Compound−DNA Complexes. All compounds were dissolved in DMSO prior to dilution with saline. The final maximum DMSO concentration in the growth medium was 2%. Stock solutions of each compound (1 mg/mL) were stored in the dark at room temperature until use. Compound−DNA complex formation was accomplished by addition of CT DNA (Calf thymus DNA) to aliquots of each of the compounds at different concentrations in TE buffer (50 mM NaCl, 10 mM Tris-HCl, 0.1 mM EDTA pH 7.4). The amount of compound added to the DNA solution was designated as r_i (the input molar ratio of Pt, Pd, or ligand to nucleotide). The mixture was incubated at 37 °C for 24 h.

Circular Dichroism Study. The CD spectra of the complex−DNA compounds (DNA concentration 20 μg/mL, $r_i = 0.10$, 0.30, and 0.50) were recorded at room temperature on a JASCO J720 spectropolarimeter with a 450 W xenon lamp using a computer for spectral subtraction and noise reduction. Each sample was scanned twice in a range of wavelengths between 220 and 330 nm. The drawn CD spectra are the means of two independent scans. The data are expressed as mean residue molecular ellipticity [θ] in deg cm^2 dmol^{-1}. The CD spectra of the complexes were subtracted from the CD spectra of each of the complex:DNA adducts by computer.

Electrophoretic Mobility Study. pB*R*322 DNA aliquots (0.25 μg/mL) were incubated in the presence of compounds in TE buffer at the molar ratio $r_i = 0.50$ for electrophoresis studies. Incubation was carried out in the dark at 37 °C for 24 h; 24 μL aliquots of complex−DNA compounds containing 0.7 μg of DNA underwent 1% agarose gel electrophoresis for 4 h at 1.5 V/cm in 0.5XTBE (45 mM Tris-borate, 1 mM EDTA pH 8.0) buffer. Gel was subsequently stained in the same buffer containing ethidium bromide (1 μg/mL). The DNA bands were viewed with a TC-312A transilluminator spectroline and the image captured by a Cohu High Performance CCD camera.

Atomic Force Microscopy. Preparation of adducts DNA−metal complexes. pB*R*322 DNA (25 μg/μL) was incubated in an appropriate volume with the required palladium and platinum concentration corresponding to the molar ratio $r_i = 0.005$. The complexes were dissolved in HEPES buffer (40 mM HEPES pH 7.4 and 10 mM $MgCl_2$). The different solutions as well as Milli-Q water were passed through 0.2 nm FP030/3 filters (Schleicher & Schuell GmbH, Germany) and centrifuged at 4000*g* several times to avoid salt deposits and provide a clear background when they were imaged by AFM. The reactions were run at 37 °C for 24 h in the dark.

Sample Preparation for Atomic Force Microscopy. Samples were prepared by placing a drop (3 μL) of DNA solution or DNA−metal complex solution onto green mica (Ashville-Schoonmaker Mica Co., Newport New, VA). After adsorption for 5 min at room temperature, the samples were rinsed for 10 s in a jet of deionized water of 18 MΩ cm^{-1} from a Milli-Q water purification system directed onto the surface with a squeeze bottle. They were then placed into ethanol−water mixture (1:1) five times and plunged three times each in ethanol (100%). The samples were blow dried with compressed argon over silica gel and then imaged in the AFM.

Imaging by Atomic Force Microscopy. The samples were imaged in a Nanoscope III Multimode AFM (Digital Instrumentals Inc., Santa Barbara, CA) operating in tapping mode in air at a scan rate of 1−3 Hz. The AFM probe was a 125-mm-long monocrystalline silicon cantilever with integrated conical-shaped Si tips (Nanosensors GmbH Germany) with an average resonance frequency $f_o = 330$ kHz and spring constant $K = 50$ N/m. The cantilever is rectangular, and the tip radius given by the supplier is 10 nm, a cone angle of 35°, and high aspect ratio. In general, the images were obtained at room temperature ($T = 23 \pm 2$ °C) and the relative humidity (RH) was typically lower than 40%.

Cell Line and Culture. The cell line used in this experiment was the human acute promyelocytic leukemia cell line HL-60 (American Type Culture Collection (ATCC)). Cells were routinely maintained in RPMI-1640 medium supplemented with 10% (v/v) heat-inactivated fetal bovine serum, 2 mmol/L glutamine, 100 U/mL penicillin, and 100 μg/mL streptomycin (Life Technologies, Inc.) in a highly humidified atmosphere of 95% air with 5% CO_2 at 37 °C.

Cytotoxicity Assay. Growth inhibitory effect of palladium and platinum complexes on the leukemia HL-60 cell line was measured by the microculture tetrazolium [3-(4,5-dimethylthiazol-2-yl)-2,5-diphenyltetrazolium bromide, MTT] assay.[51] Briefly, cells growing in the logarithmic phase were seeded into 96-well microtiter plates in 100 μL of the appropriate culture medium at a plating density of 1×10^4/well. Following the addition of different complex concentrations to quadruplicate wells, plates were incubated at 37 °C for 24 or 72 h. Aliquots of 20 μL of MTT solution were then added to each well. After 3 h the color formed was quantitated by a spectrophotometric plate reader (BIO-TEK INSTRUMENTS, INC.) at a wavelength of 490 nm. The percentage cell viability was calculated by dividing the average absorbance of the cells treated with a palladium or platinum complex by that of the control; % cell viability vs drug concentration (logarithmic scale) was plotted to determine the IC_{50} (drug concentration at which 50% of the cells are viable relative to the control) with its estimated error derived from the average of three trials.

In Vitro Apoptosis Assay. Induction of apoptosis in vitro by complexes **1**−**11** and cisplatin was determined by a flow cytometric assay with Annexin V-FITC[52] using an Annexin V-FITC Apoptosis Detection Kit (Roche). Exponentially growing HL-60 cells in six-well plates (5×10^5 cells/well) were exposed to IC_{50} concentrations of cisplatin or complexes **1**−**11** for 24 h. Afterward the cells were subjected to staining with the Annexin V-FITC and propidium iodide as detailed by the manufacturer. The amount of apoptotic cells was analyzed by flow cytometry (BD FACSCalibur).

Acknowledgment. Financial support of this work by the Dirección General de Investigación del Ministerio de Ciencia y Tecnología (Project Nos. BQU2001-0979-C02-01 and Bio2001-2046), Spain, and the Fundación Séneca de la Comunidad Autónoma de la Región de Murcia (Project No. PI-72-00773-FS-01) is acknowledged. The authors thank Dra. María José Prieto (EF and AFM), Dra. Francisca García (Cell Culture Facility), and Manuela Costa (Cytometry Facility) for technical assistance.

Supporting Information Available: X-ray crystallography data for complexes **1**, **7**, **8**, and **11**. This material is available free of charge via the Internet at http://pubs.acs.org.

IC0502372

(51) Mosmann, T. *J. Immunol. Methods* **1983**, *65*, 55.
(52) Vermes, I.; Haanen, C.; Steffens-Nakken, H.; Reutelingsperger, C. *J. Immunol. Methods* **1995**, *184*, 39.